GEOPHYSICAL RESEARCH LETTERS, VOL. 27, NO. 9, PAGES 1259-1262, MAY 1, 2000

Kelvin wave and Rossby wave interaction in the extratropical-tropical Pacific

Lixin Wu Zhengyu Liu
Center For Climate Research, University of Wisconsin-Madison

Harley E. Hurlburt
Naval Research Laboratory, Stennis Space Center, Mississippi

Abstract The adjustment of the equatorial Pacific thermocline to an initial extratropical thermocline anomaly is studied using analytical and high-resolution (1/16°) primitive equation numerical models. It is found that the fast adjustment due to the coastal Kelvin wave and equatorial Kelvin and Rossby waves, and the slow adjustment due to the eastern boundary planetary wave play important roles in the redistribution of the initial anomalous mass, thereby determining the phase and magnitude of the equatorial thermocline transition induced by the initial extratropical thermocline transition. For a given extratropical anomaly, both analytical and numerical models show that the equatorial thermocline transition occurs about 2-5 years later, and the magnitude is about 5 - 10% of the initial anomaly. The mean circulation in the North Pacific intensifies the transition of the equatorial thermocline and reduces the phase-lag of extratropical-tropical thermocline transition.

1. Introduction

Recent interest in the interaction of Kelvin waves and low frequency planetary waves is motivated by their roles in (1) extratropical-tropical upper ocean interaction at interannual to interdecadal time scales (Godfrey, 1975; Jacobs et al., 1994; Lysne et al., 1997), (2) the extra-equatorial and equatorial regions associated with the onset of El Niño – Southern Oscillation (ENSO) events (Cane and Sarachik, 1977; McCreary,1983; Battisti, 1989; Kessler 1991) , (3) the adjustment of global sea level due to the redistribution of heat within the ocean from the high latitudes to the equator associated with global greenhouse warming (Hsieh and Bryan, 1996), and (4) formation of deep ocean circulation (Wajsowicz and Gill, 1986; Kawase, 1987).

In this letter, the adjustment of the equatorial Pacific thermocline to an initial thermocline anomaly in the extratropics is studied in light of Kelvin waves and Rossby waves. This is motivated by a recent general circulation model (GCM) study on the impact of the extratropical Pacific on equatorial variability by Lysne et al. (1997), where they found that the time lag between the central North Pacific and the tropical warm transition is only about 3-5 years, much shorter than the time it takes for the subducted warm anomaly to reach the equatorial region. This relatively short time lag suggests that, in addition to the subduction process (McCreary and Lu, 1994; Liu and Philander, 1995), some wave mechanisms are responsible for the transmission of warm anomalies from the extratropics to the equator. This is the main focus of this letter. We will show *quantitatively* the important role of coastal Kelvin waves and equatorial Kelvin and Rossby waves, and eastern boundary planetary waves on the extratropical-tropical communication by means of a simple theory and a high resolution primitive equation numerical model.

Paper number 1999GL002368.
0094-8276/00/1999GL002368$05.00

2. Results

The numerical ocean model used is a vertically integrated primitive equation formulation developed at the Naval Research Laboratory (Wallcraft, 1991). The version used here for the North Pacific is the same as that used in Hurlburt et al. (1996) except that all of the simulations performed here are 1.5 layer reduced gravity. The mean upper layer thickness is 500 m. In the model, the initial extratropical thermocline anomaly is assumed to have a cosine form in both the meridional and zonal directions:

$$\eta(\phi,\theta) = \eta_o \cos(\pi(\phi-\phi_c)/\phi_p)\cos(\pi(\theta-\theta_c)/\theta_p) \qquad (1)$$

in which (ϕ_c,θ_c) is the center of the packet, θ_p,ϕ_p are the meridional and zonal dimensions, and η_o is the initial amplitude. The initial velocity field is calculated by the relations of geostrophic balance. In the control experiment, the center of the wave packet is set at (180°, 30°N). The size of the wave patch is chosen as $\phi_p = 60^o, \theta_p = 20^o$, which is much larger than the deformation radius.

The evolution of the initial SSH anomaly is illustrated by Figures 2a-d. Before the wave packet arrives at the western boundary, the propagation is mostly westward at a rate controlled by the non-dispersive relation. The southern part of the patch propagates faster than the northern part, in accordance with the differing local deformation radius. At the end of the first year, the wave front first impinges on the eastern coast of Japan at 35°N, establishing a clockwise coastal Kelvin wave current within a short time of about 12 days, with a positive sea surface height anomaly along the coast of Japan. On the western coast of Japan, a Rossby wave is radiated and propagates westward in the Japan Sea. As the front of the southern part of the initial anomaly impinges on the eastern coast of China, it generates an equatorward coastal Kelvin wave which passes through the Luzon Strait and travels anticlockwise along the coast of the South China Sea. Before exiting into the Sulu Sea through Mindoro Strait, the Kelvin wave sheds mass from the western coast of Palawan into the South China Sea in the form of a westward planetary wave. On the eastern boundary, the equatorial Kelvin wave is reflected by shedding most of its mass and energy into a westward equatorial Rossby wave. The Rossby wave then reflects as an equatorial Kelvin wave and so forth. These reflections of equatorial waves rapidly build up a quasi-basin mode (Cane and Moore, 1981). A small amount of mass leaks out poleward along the eastern boundary in each hemisphere as a coastal Kelvin wave. In the extratropics, due to the shrinking of deformation radius, the Kelvin wave sheds its mass into the interior by

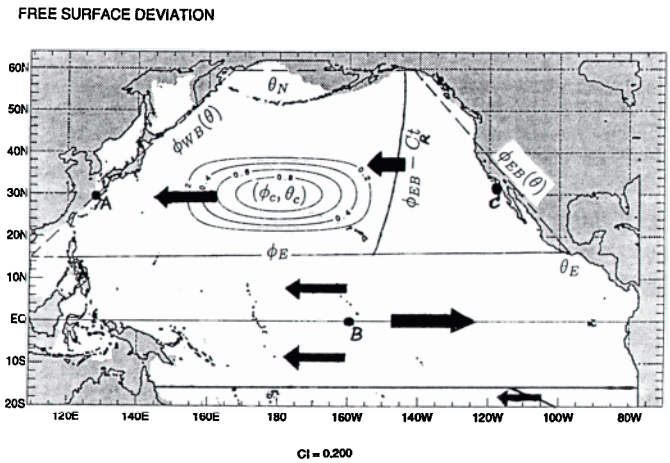

Figure.1: The basin geometry of the Pacific Ocean model. The 200-m isobath defines the mode land/sea bounday except the straits connecting the Sea of Japan with the Pacific Ocean. Various solution regimes for the adjustment process are plotted. The coordinates of the diagnosed points (•) are: A(128E, 30N), B(160W, 0), C(117.4W, 32N). The dashed lines represent idealized coastlines used in the theoretical model, with $\phi_{WB}(\theta)$ denoting the western boundary, $\phi_{EB}(\theta)$ the eastern boundary, and θ_N the northern boundary. The small marginal seas are ignored in the theoretical model.

generating an eastern boundary planetary wave. The eastern boundary planetary wave redistributes most of the initial anomalous mass throughout most of the Pacific and thereby significantly reduces the amplitude of the sea surface height anomaly. At a decadal time scale, a nearly uniform sea surface height can be reached over the entire basin.

The evolution of the monthly mean SSH associated with the transition of the equatorial thermocline is plotted on the equator (h_B) and eastern boundary (h_C) (Fig. 3a). For comparison, the SSH near to the western boundary (h_A) at the latitude of θ_C is also plotted, representing the incident wave packet. Both the equatorial Kelvin wave and eastern boundary Kelvin wave show virtually the same phase and amplitude. The planetary wave impinges on the western boundary after about one year, peaks after about 3 years, and ends after about 6 years. The equatorial Kelvin wave initiates at year 1.3 and peaks at about year 4.5, which is about 1.5 years later than the peak time of the incident wave. The amplitude is about 6% of the initial extratropical anomaly. The small amplitude is due to the mass spreading over a larger area, which includes a large equatorial region and eastern boundary planetary wave region. The fast adjustment in the large equatorial region is dominant as can be seen in the history of mass distribution.

The time series of mass (normalized by the initial mass) in the equatorial region, eastern boundary planetary wave region (EBP), western boundary incident planetary wave (IP) and western Pacific marginal seas are plotted in Fig. 3b. The definition of these regions can be found in Fig. 1. The latitudinal width θ_E of the equatorial region is estimated by the relation: $\phi_P / C_R(\theta_C) = \phi_E / C_R(\theta_E)$, in which C_R is the zonal (ϕ) speed of the planetary wave. Physically, it means that the waves within this band can cross the basin by the time the initial extratropical planetary wave packet passes the western boundary, and therefore

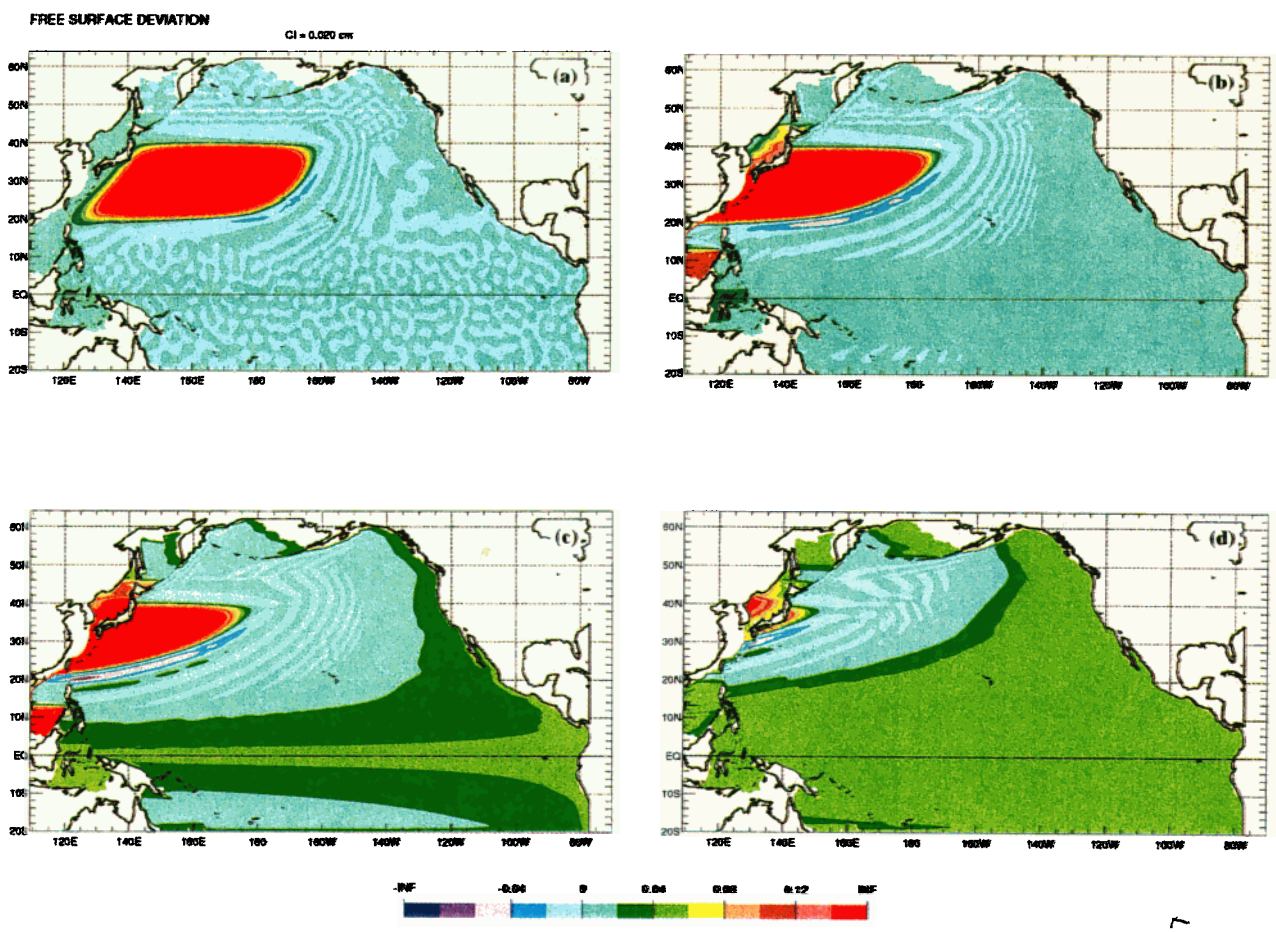

Figure.2: Four snapshots of sea surface height for an initial extratropical SSH anomaly. (a) T=1 year, (b) T=3 years, (c) T= 4 years, (d) T=6.6 years. The contour interval is 0.02, normalized by the initial amplitude. There is no mean flow.

can more efficiently participate in the fast adjustment process (Liu et al., 1999). With the model parameters, θ_E is about 16°. The mass evolution diagram clearly shows that much of the western boundary incident mass is rapidly injected into the equatorial wave band, while the mass in the EBP region grows slowly and becomes comparable to the equatorial wave band at a later stage. The diagram also shows that the mass in the western marginal seas is negligible, even though the sea surface height may not be small (Fig. 2). So the dominant mass balance can be simply written as $M_{IP}(t)+M_{EQ}(t)+M_{EBP}(t)=M_0$, where M_o is the mass of the initial anomaly. The mass of the incident planetary wave can be written as:

$$M_{IP}(t)=\int_{\theta_c-\theta_p/2}^{\theta_c+\theta_p/2}\int_{\phi_{WB}(\theta)}^{\phi_c+\phi_p/2-C_R t}\eta(\theta,\phi+C_R t)R\cos\theta d\theta d\phi \qquad (2)$$

where $C_R=g'H/2\Omega R\sin^2\theta$, and Ω and R are the rotation speed and the radius of the earth.

In the equatorial Pacific, the mass can be written as $M_{EQ}(t)\approx K(t)S_{EQ}$, where S_{EQ} is the area of the fast adjustment equatorial band within $(-\theta_E,\theta_E)$, and K(t) is the amplitude of the Kelvin wave.

In the eastern Pacific, the mass spreads into the interior by the EBP,and can be derived as: $M_{EBP}(t)=X\int_0^t K(t')dt'$, in which $X=\int_{\theta_E}^{\theta_N}R^2C_R\cos\theta d\theta$.

The mass conservation equation can be differentiated to yield an ordinary differential equation about the amplitude of the Kelvin wave and explicitly solved with the initial condition of

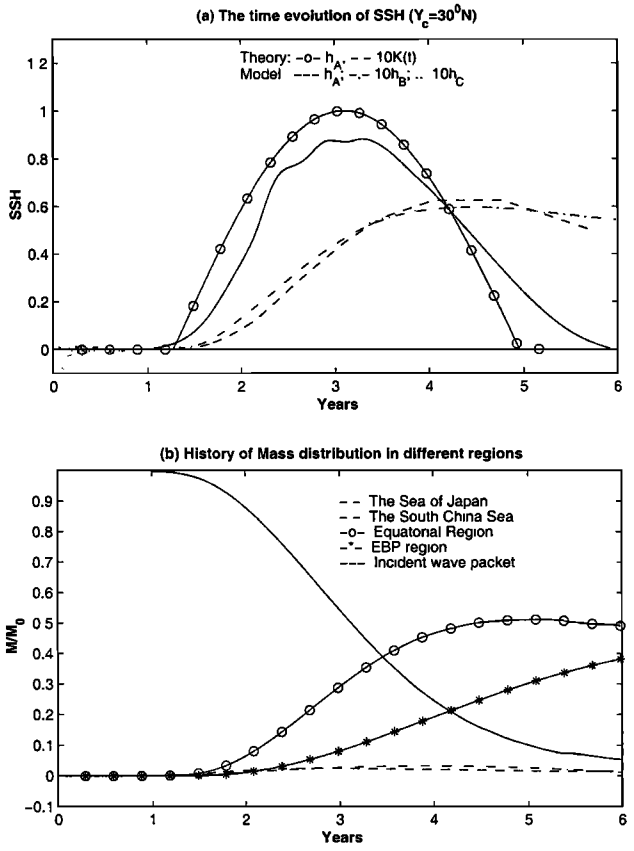

Figure.3 (a): Evolution of the amplitude of the equatorial Kelvin wave (h_B), eastern coastal Kelvin wave (h_C) and western boundary incident planetary wave (h_A) for the experiment in Figure 2. The theoretical solutions are also plotted. (b): Evolution of mass in different regions is plotted. Both the mass and amplitude are normalized by the initial perturbation quantity.

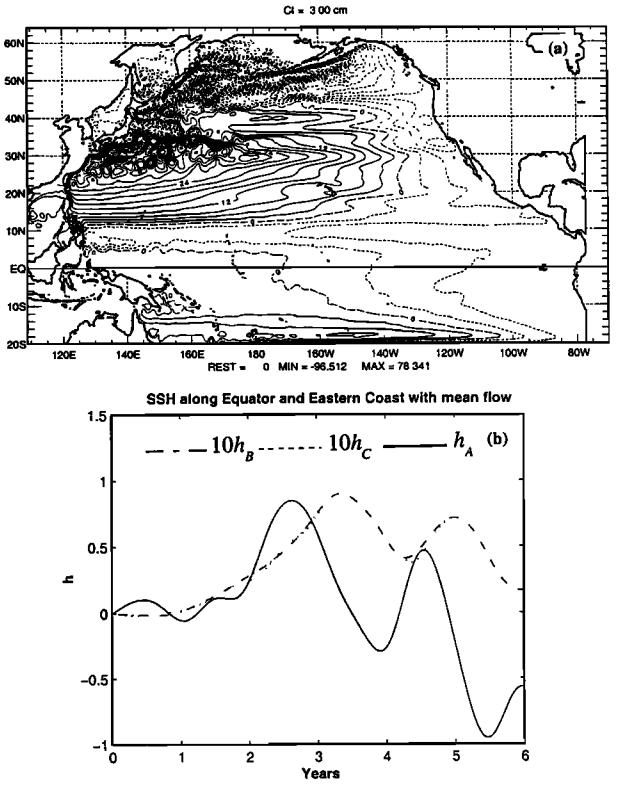

Figure.4 (a): Five-year mean sea surface height from a reduced gravity primitive equation simulation using the 1/16° NRL Pacific Ocean model. It was driven for 50 years by annual-mean Hellerman-Rosenstein wind stresses. The contour interval is 3.00cm. The maximum sea surface height in the subtropical gyre is 78.34cm. (b): Evolution of the amplitude of the equatorial Kelvin wave (h_B) , eastern coastal Kelvin wave (h_C) and western boundary incident planetary wave (h_A) in the presence of the mean circulation. The initial anomaly has the same size and location as in Fig.2, but the magnitude is 10% of the mean surface height. The amplitude is normalized by the initial perturbation amplitude.

K(0)=0. The analytical solution is also plotted in the SSH diagram of the numerical model simulation (Fig. 3a). The incident planetary wave calculated by the long wave approximation agrees quite well with the numerical model. The amplitude first increases to its maximum at the peak time T_M = 3.2 years, then decreases to zero at the ending time T_E = 5 years by which time the wave packet passes the western boundary. A weaker amplitude and longer ending time in the numerical model may be caused by the presence of the western boundary layer and wave dispersion. But, the evolution of the equatorial thermocline predicted by the analytical model closely resembles the numerical simulation. It is noted that both the phase and amplitude of the equatorial Kelvin wave are consistent with the finding in the GCM study of Lysne et al. (1997), where they found the equatorial warm transition occurs 3-5 years later than the extratropical warm transition, and the amplitude is about 5% of the initial extratropical anomaly (See their Figure 3 (a) and (d)).

The preceding theory is based on the linear wave approximation, where it is assumed that there is no interaction between the mean flow advection and the imposed anomaly. It will be shown that the linear results are robust even in the presence of the Kuroshio Current. To get a more realistic mean flow, the model is spun up with the annual mean Hellerman-Rosenstein wind for 50 years from the initial quiescent state to a quasi-equilibrium state. The last 5 years mean sea surface height is plotted in Figure 4(a). The high resolution enables the model to obtain a more realistic Kuroshio/Oyashio current system. After the spin up, two parallel runs are performed. First, without any modification, we run the model for another 6 years as the control run. Second, we impose a SSH anomaly with the same size and

location as the previous linear experiment, and run the model for another 6 years. The amplitude of the imposed anomaly is 10% of the mean sea surface height. The response induced by the initial perturbation can be detected by the difference of these two runs at each time step.

The evolutions of the equatorial Kelvin wave, eastern boundary Kelvin wave and western boundary incident wave packet (normalized by the amplitude of the initial anomaly and smoothed by spline method) are plotted in Figure 4(b). The incident planetary wave peaks at year 2.6, ends at year 3.4 and bounces back at a later stage due to the interaction with the boundary current. Compared with the linear experiment, in the interior the propagation of the wave packet seems to be not affected by the mean advection. But, as the wave packet impinges on the western boundary (after about one year), it crosses the basin rapidly within about 2 years, which is almost half of the linear case. This may be attributed to the strong mean advection near the Kuroshio. The fast crossing of the extratropical western boundary incident wave only allows the planetary waves which are radiated at a lower latitude from the eastern boundary, to cross the basin before its trail crosses the western boundary. This reduces the area of the fast equatorial adjustment process, therefore increases the magnitude of the equatorial thermocline transition. It can be seen that the peak amplitude of the equatorial Kelvin wave now is 0.09, about 1.5 times the linear experiment amplitude. The eastern boundary SSH also shows the same phase and magnitude as the equatorial SSH. It seems that the Kelvin wave is less affected by the mean boundary current advection due to its rapid propagation along the boundary (3.64m/s contrast to 1.3m/s of the model Kuroshio Current).

3. Summary

The adjustment of the equatorial thermocline to an initial extratropical planetary wave packet is *quantified* using analytical and high-resolution primitive numerical models. It is found that the fast adjustment due to the coastal Kelvin wave and equatorial Kelvin and Rossby waves, and slow adjustment due to the eastern boundary planetary wave play a crucial role in the redistribution of the initial mass anomaly, and thus determine the phase and magnitude of the equatorial thermocline transition in response to the extratropical transition. For a given extratropical anomaly, both the analytical and numerical models show that the equatorial thermocline transition occurs about 2-5 years later, and the magnitude is about 5-10% of the initial extratropical anomaly. The presence of the mean circulation intensifies the transition of the equatorial thermocline and reduces the extratropical-tropical phase lag.

It should be pointed out that the mean upper layer thickness in the model is consistent with the extratropical mean thermocline, but is unrealistic in the equatorial Pacific where the thermocline depth is about half of the model layer thickness. In reality, it is believed that for the same initial extratropical anomaly, the modulation of the equatorial thermocline can be stronger than the model prediction in the fact that the first baroclinic equatorial Kelvin and Rossby waves propagates slower than that in the model, leading to a narrower fast adjustment equatorial band.

The relative amplitude and phase of the equatorial thermocline modulation may not critically depend on the sign and amplitude of the initial extratropical thermocline anomaly. In a series of idealized experiments with a rectangular basin and without mean advection, an increase of the initial amplitude of extratropical thermocline anomaly does not cause a change of the relative amplitude and phase of the equatorial thermocline modulation. This is because that the short Rossby wave adjustment on the western boundary contributes less to the basin mass balance. A negative extratropical anomaly does not change the process of wave adjustment of the basin mass balance even the directions of the currents are reversed, therefore the amplitude and phase of the equatorial thermocline anomaly resembles those induced by a positive extratropical anomaly. In the presence of mean advection, a strong initial extratropical anomaly may modulate the mean flow, which produces a nonlinear feedback to the wave propagation near the boundary and thus affects the adjustment of the equatorial thermocline. More detailed theoretical analyses and model experiments on how the mean flow advection influences the Kelvin-Rossby wave interaction are currently underway

Acknowledgments We would like to thank E. J. Metzger and A. J. Wallcraft for their help in the set up of the Navy layered Pacific Ocean model. The comments from two anonymous reviewers are helpful to improve the quality of the paper. This work was supported by ONR, NSF and NOAA. The numerical experiment was performed on the NAVO CRAY T3E at Stennis Space Center, Mississippi under a grant of computer time from the DoD High Performance Computing Modernization Office.

References

Battisti, D. S, 1989: On the role of off-equatorial oceanic Rossby waves during ENSO. J. *Phys. Oceanogr.*, 19, 551-559.

Cane, M. A. and E. S. Sarachik, 1977: Forced baroclinic ocean motions. II. The linear equatorial bounded case. *J. Mar. Res.*, 35, 395-432.

Cane, M. A. and D. Moore, 1981: A note on low frequency equatorial basin modes. *J. Phys. Oceanogr.*, 11, 1578-1584.

Godfrey, J. S. 1975: On ocean spindown I: A linear experiment. *J. Phys. Oceanogr.*, 5, 399-409.

Hellerman, S. and M. Rosenstein, 1983: Normal monthly wind stress over the world ocean with error estimates. *J. Phys. Oceanogr.*, 13, 1093-1104.

Hsieh, W. W. and K. Bryan, 1996: Redistribution of sea level rise associated with enhanced greenhouse warming: a simple model study. *Climate Dynamics*, 12, 535-544.

Hurlburt, H. E., A. J. Wallcraft, W. J. Schmitz Jr., P. J. Hogan and E. J. Metzger, 1996: Dynamics of the Kuroshio/Oyashio current system using eddy-resolving models of the North Pacific Ocean. *J. Geophys. Res.*, 101, 941-976.

Jacobs, G. A., H. E. Hurlburt, J. C. Kindle, E. J. Metzger, J. L. Mitchell, W. J. Teague and A. J. Wallcraft, 1994: Decade-scale trans-Pacific propagation and warming effects of an El Nino anomaly. *Nature*, 370, 360-363.

Kawase, M., 1987: Establishment of deep ocean circulation driven by deep-water production. *J. Phys. Oceanogr.*, 17, 2294-2317.

Kessler, W. S., 1991: Can reflected extra-equatorial Rossby waves drive ENSO? *J. Phys. Oceanogr.*, 21, 444-452.

Liu, Z., L. Wu and E. Bayler, 1999: Rossby wave – coastal Kelvin wave interaction in the extratropics I: Low frequency adjustment in a closed basin. *J. Phys. Oceanogr.*, 29,2382-2404.

Liu, Z. and S. G. Philander, 1995: How different wind stress patterns affect the tropical-subtropical circulations of the upper ocean, *J. Phys. Oceanogr.*, 25, 449-461..

Lysne, J., P. Chang, and B. Giese, 1997: Impact of the extratropical Pacific on equatorial variability. *Geophys. Res. Lett.*, 24, 2589-2592.

McCreary, J., 1983: A model of the tropical ocean-atmosphere interaction. *Mon. Wea. Rev.*, 111, 370-387.

McCreary, J. P. and P. Lu, 1994: Interaction between the subtropical and the equatorial ocean circulations: the subtropical cell. *J. Phys. Oceanogr.*, 24, 466-497.

Wallcraft, A. J. 1991: The Navy layered ocean model users guide. NOARL Report 35, Naval Research Laboratory, Stennis Space Center, MS, 21pp.

Wajsowicz, R. C. and A. E. Gill, 1986: Adjustment of the ocean under buoyancy forces. Part I: The role of Kelvin waves. *J. Phys. Oceanogr.*, 16, 2097-2114.

L. Wu, Z.Liu Department of Atmospheric and Oceanic Science and Center For Climate Research, University of Wisconsin-Madison, 1225, W. Dayton St., Madison, WI 53706 (e-mail: lxw@tuna.meteor.wisc.edu)

Hurlburt, H.E. Naval Research Laboratory, Code 7323, Stennis Space Center, MS 39529.

(Received June 28,1999; Revised December 06,1999; Accepted January 21, 2000)